MRS Advances © 2018 Materials Research Society
DOI: 10.1557/adv.2018.117

Nanopatterning Hexagonal Boron Nitride with Helium Ion Milling: Towards Atomically-Thin, Nanostructured Insulators

S. Matt Gilbert[1,2,3], Stanley Liu[1,3], Gabe Schumm[1,3], Alex Zettl[1,2,3]

[1] *Department of Physics, University of California, Berkeley, CA, 94720*

[2] *Materials Science Division, Lawrence Berkeley National Laboratory, Berkeley, CA, 94720*

[3] *Kavli Energy Nanosciences Institute, Berkeley, CA, 94720*

ABSTRACT

In this report, we demonstrate the use of helium ion milling for the controllable fabrication of nanostructures in few-layer hexagonal boron nitride (h-BN). Using the direct-write lithographic capabilities of a scanning helium ion microscope (HIM), nanopores with diameters as small as 4 nm and nanoribbons with widths of 3 – 10 nm are etched from suspended h-BN sheets. This ability to pattern h-BN sheets with high-throughput and sub-10 nm precision paves the way for future studies that make use of atomically-thin, nanostructured insulators such as those needed for nanopore sequencing and patterned van der Waals heterostructures.

INTRODUCTION

Few-layer hexagonal boron nitride (h-BN) has emerged as an important material in the study of heterostructures of two-dimensional (2D) materials [1-3], and its many unique properties suggest a variety of stand-alone applications [4-7]. As an atomically-thin and chemically-inert sp^2 hybridized insulator, h-BN is an ideal substrate and encapsulation layer for graphene and transition metal dichalcogenides (TMDs) [1,3,8,9]. Its flat surface and lack of dangling bonds reduce substrate-induced scattering for encapsulated 2D materials, and its impermeability prevents oxidation of these encapsulated layers [7, 8, 10, 11].

The ability to pattern and etch h-BN has been explored for a variety of purposes to aid in its role in graphene electronics. Patterned h-BN has been demonstrated as a growth template for CVD graphene [12]. Stacks of h-BN/graphene/h-BN have been etched to create edge contacts for the encapsulated graphene [11, 13]. Holes through h-BN stacked on graphene have been used to create point contacts for the graphene [14]. Moreover, nanostructures in insulating materials are being studied for their role in the production of superlattices in two-dimensional materials; the ability to pattern and etch h-BN for this purpose could enhance the results in the existing literature by moving the electronic 2D material closer to the periodic potential [15].

The patterning and etching of h-BN has also been studied for several stand-alone applications. Nanopores etched in h-BN have been shown to confer several advantages for DNA sequencing over their graphene counterparts [4, 16]. h-BN nanoribbons etched from boron nitride nanotubes have also been explored due to their interesting magnetic and electronic properties [17-19].

Here we demonstrate the use of helium ion milling for the controlled fabrication of nanostructures in few-layer h-BN. Specifically, we show using a direct-write lithographic system that nanopores with diameters as small as 4 nm and ribbons with 3-10 nm width can be attained – roughly a factor of 5 smaller than what can be made by conventional electron beam lithography [20]. This method of nanopore formation achieves comparable sizes to milling in a transmission electron microscope (TEM) but at a much higher throughput [4, 21-24].

The high precision and rapid rate of pore production suggests that this method may be useful for scaling up the fabrication of nanopore sensors, producing point contacts for h-BN encapsulated devices, or for testing applications that require a large number of holes on a sample such as water desalination[25, 26] or dielectric superlattices [15]. The ability to produce

sub-10 nm ribbons demonstrates that this technique could be a straightforward method for studying the properties of h-BN nanoribbons. Furthermore, the demonstration ribbons at these sizes shows that other h-BN nanostructures can be created with minimal damage even at these small dimensions, allowing for the production h-BN deposition/etch masks, beams and cantilevers, and patterned dielectric layers.

EXPERIMENT AND RESULTS

Few-layered h-BN used for the suspended structures in this study was prepared by chemical vapor deposition (CVD) on copper following references [16] and [27]. The synthesis method in this work produces 3-5 layers of h-BN, ideal for creating near atomically-thin yet mechanically-stable suspended films. To prepare for the CVD growth, 1 cm x 4 cm copper foils are rinsed in glacial acetic acid for 10 minutes followed by 3 deionized water baths. A foil is then loaded into a tube furnace and annealed for 2 hours at 1020° C under a gas flow of 300 sccm of Ar and 100 sccm of H_2 at 1 Torr. After the 2 hours of annealing, the Ar gas flow is turned off and 100 mg of ammonia-borane powder (Sigma Aldrich 97%), located in an upstream one-end sealed quartz tube, is heated to 80° C for 30 minutes, allowing the BN precursor to diffuse to the copper catalyst where h-BN grows on the surface. The ammonia-borane is then cooled quickly to end the growth while the copper foil cools slowly at a rate of 10° C/min.

Suspended samples of h-BN are then prepared by direct transfer as described in reference [28]. h-BN coated copper foils are cut into 4 mm x 4 mm pieces and a drop of isopropanol is used to adhere a holey-carbon TEM grid to the h-BN surface. The stack is then floated (grid on top) in 10% weight-per-volume sodium persulfate solution and underlying copper is dissolved, leaving behind an h-BN coated holey-carbon grid. The sample is removed from the sodium persulfate, floated in deionized water briefly to remove any residual copper etchant, and then is ready for use.

h-BN nanostructures are prepared from the suspended sheets by locally etching with the focused helium beam of a Zeiss ORION NanoFab helium ion microscope (HIM). The microscope is operated at 25 kV with a beam current of ~1 pA. Features to be etched are defined using a direct-write lithography software that precisely controls the position of the beam and dose delivered. We find that it is necessary to use suspended h-BN in order to prevent the re-deposition of etched species on a substrate. In order to protect the sample from uncontrolled etching, imaging of the h-BN using the HIM is minimized;[29, 30] therefore, characterization is performed *ex situ* by TEM using a JEOL 2010 operated at 80 kV.

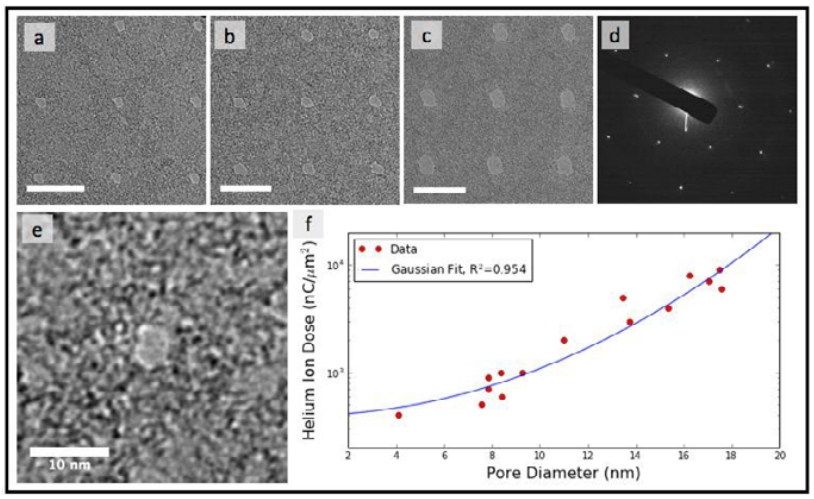

Figure 1: a.)-c.) Arrays of holes in h-BN produced by spot exposures at a.) 500, b.) 1000, and c.) 5000 nc/μm^2 as imaged by TEM d.) Selected area electron diffraction taken on a hole array with spot exposures of 1000 nc/μm^2. e.) A single nanopore produced by a spot exposure with 400 nc/μm^2 irradiation as imaged by TEM.. f.) Average pore diameter versus helium ion dose for 6x6 arrays of holes produced by spot exposures ranging from 400 - 10000 nc/μm with an overlaid Gaussian fit with $R^2 = 0.954$.Scale bars are: a.) - c.) 50 nm, e.) 10 nm.

To explore the relationship between helium ion dose and minimum etch-feature size, the suspended h-BN sheets are irradiated using point exposures at varying doses. 6 x 6 arrays of points, spaced by 60 nm, are exposed (with a constant ion dose for all points) using the focused helium beam. Doses for each array range from 100 – 10,000 nc/μm^2 over a nominal probe size of 0.5 nm in diameter, typically requiring less than 1 second (up to 1000 nc/μm^2) to 10 seconds (up to 10,000 nc/μm^2) per spot exposed.

Figure 1(a)-(d) show the resulting pores formed by the helium ion point exposures. The sizes of all of the pores in a 6 x 6 array are measured and averaged as plotted in Figure 1(f). Similar to previous results that investigate the etching of graphene using helium ion milling, we find that the variation of the size of the h-BN pores with total ion dose can be attributed to the Gaussian profile of the beam [30, 31]. This is confirmed by the Gaussian dependence of the required helium ion dose versus pore radius shown in Figure 1(f). Figure 1(e) shows selected area electron diffraction (SAED) from an irradiated region; the regular crystal structure without strong presence of rings suggests that the h-BN is not substantially disordered by the etching.

In this study, the smallest pores formed were approximately 4 nm as shown in Figure 1(e). Pores this size were formed by irradiating the sample at 400 nC/μm^2. At spots exposed with lower doses, no pore formation was observed. These 4 nm pores are highly irregular in geometry and seem more elliptical than circular (major diameter = 5 nm, minor diameter = 3 nm) likely due to either beam/sample drift or beam stigmation. The irregular geometry suggests that further characterization and optimization is required to understand the edges. Nanopores of this size in MoS_2 have been previously used to discern single nucleotides, suggesting that this too is possible with the h-BN pores formed in this way [22].

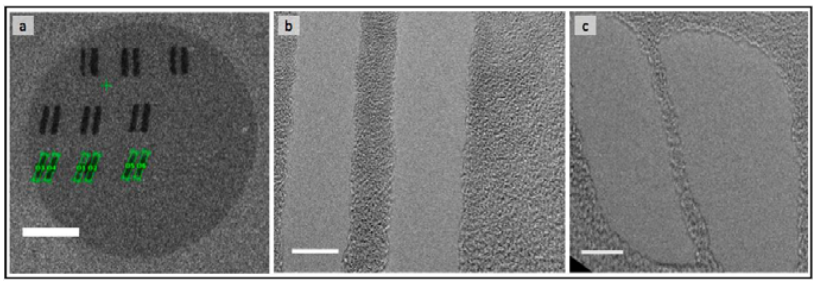

Figure 2: a.) A HIM image of rows of 70 x 15 nm h-BN ribbons with different rotation angles. The h-BN region is suspended over the center circle while the outer region is backed by holey-carbon. The numbered rectangles overlaid on the bottom row depict the region exposed to produce the ribbons as shown in the computer aided design software. b.) A TEM image of a 7 nm width h-BN nanoribbon (center) next to a 30 nm width ribbon (right). c.) A TEM image of a 3 nm width h-BN nanoribbon. Scale bars are: a.) 150 nm, b.) and c.) 10 nm.

h-BN ribbons were formed by irradiating two identical rectangular regions on either side of a narrow strip as shown in Figure 2(a). By varying the distance between the etched shapes, the width of the ribbon is tuned. A total dose of 1 nc/μm^2 was found to be the minimum dose to fully etch the selected region and was therefore used to minimize damage to the h-BN ribbon. As shown in Figure 2(b), sub-10 nm width ribbons can be fabricated in this way without incurring significant damage; this is reflected by the lack of obvious differences between the 7 nm width ribbon (left) and the center of the 30 nm width ribbon (right).

By further irradiating the ribbons after etching by imaging the sample continuously with the HIM, the ribbons can be whittled down. This implies that the edge is more susceptible to etching than the rest of the suspended sample. Using this method, ribbons can be whittled to less than 3 nm as shown in Figure 2(c). However, these whittled ribbons appear damaged; this can be seen in Figure 2(c) in which the shape of the ribbon is irregular and the edges are not straight as would be expected for a crystalline edge as in reference [16]. Further characterization by high-resolution TEM is necessary to probe the extent of this damage.

CONCLUSION

We have demonstrated that helium ion milling can be used to controllably fabricate sub-10 nm nanopores and nanoribbons in h-BN. With its high throughput and precision, this technique promises to advance studies requiring large numbers of nanostructures in an insulating layer such as those needed for nanopore arrays for DNA sequencing and for etched layers in van der Waals heterostructures.

ACKNOWLEDGMENTS

This work was supported in part by the Director, Office of Science, Office of Basic Energy Sciences, Materials Sciences and Engineering Division, of the U.S. Department of Energy under Contract No. DE-AC02-05-CH11231, within the sp2-Bonded Materials Program (KC2207) which provided for TEM characterization, and within the Nanomachines Program (KC1203) which provided for methodology for membrane suspension; by the Department of Defense, Defense Threat Reduction Agency under Grant No. HDTRA1-15-1-0036, which provided for He-beam irradiation (the content of the information does not necessarily reflect the position or the policy of the Federal Government, and no official endorsement should be inferred); and by the National Science Foundation under Grant No. DMR-1206512, which provided for additional structural characterization of the pristine membranes. SMG acknowledges support from the National Science Foundation Graduate Fellowship Program.

References

1. W. Gannett, W. Regan, K. Watanabe, T. Taniguchi, M.F. Crommie, and A. Zettl, Appl. Phys. Lett. **98**, 242105 (2011).
2. C.R. Dean, A.F. Young, I. Meric, C. Lee, L. Wang, S. Sorgenfrei, K. Watanabe, T. Taniguchi, P. Kim, K.L. Shepard, and J. Hone, Nat. Nanotechnol. **5**, 722 (2010).
3. X. Cui, G.-H. Lee, Y.D. Kim, G. Arefe, P.Y. Huang, C.-H. Lee, D.A. Chenet, X. Zhang, L. Wang, F. Ye, F. Pizzocchero, B.S. Jessen, K. Watanabe, T. Taniguchi, D.A. Muller, T. Low, P. Kim, and J. Hone, Nat. Nanotechnol. **10**, 534 (2015).
4. Z. Zhou, Y. Hu, H. Wang, Z. Xu, W. Wang, X. Bai, X. Shan, and X. Lu, Sci. Rep. **3**, 13770 (2013).
5. O. Ergen, S.M. Gilbert, T. Pham, S.J. Turner, M.T.Z. Tan, M.A. Worsley, and A. Zettl, Nat. Mater. **16**, (2017).
6. T.T. Tran, K. Bray, M.J. Ford, M. Toth, and I. Aharonovich, Nat. Nanotechnol. **11**, 37 (2015).
7. Z. Liu, Y. Gong, W. Zhou, L. Ma, J. Yu, J.C. Idrobo, J. Jung, A.H. MacDonald, R. Vajtai, J. Lou, and P.M. Ajayan, Nat. Commun. **4**, ncomms3541 (2013).
8. G.-H. Lee, X. Cui, Y.D. Kim, G. Arefe, X. Zhang, C.-H. Lee, F. Ye, K. Watanabe, T. Taniguchi, P. Kim, and J. Hone, ACS Nano **9**, 7019 (2015).
9. G. Lu, T. Wu, Q. Yuan, H. Wang, H. Wang, F. Ding, X. Xie, and M. Jiang, Nat. Commun. **6**, (2015).
10. X. Chen, Y. Wu, Z. Wu, Y. Han, S. Xu, L. Wang, W. Ye, T. Han, Y. He, Y. Cai, and N. Wang, Nat. Commun. **6**, 7315 (2015).
11. F. Pizzocchero, L. Gammelgaard, B.S. Jessen, J.M. Caridad, L. Wang, J. Hone, P. Bøggild, and T.J. Booth, Nat. Commun. **7**, 11894 (2016).
12. Z. Liu, L. Ma, G. Shi, W. Zhou, Y. Gong, S. Lei, X. Yang, J. Zhang, J. Yu, K.P. Hackenberg, A. Babakhani, J.-C. Idrobo, R. Vajtai, J. Lou, and P.M. Ajayan, Nat. Nanotechnol. **8**, 119 (2013).
13. L. Wang, I. Meric, P.Y. Huang, Q. Gao, Y. Gao, H. Tran, T. Taniguchi, K. Watanabe, L.M. Campos, D.A. Muller, J. Guo, P. Kim, J. Hone, K.L. Shepard, and C.R. Dean, Science **342**, 614 (2013).
14. C. Handschin, B. Fülöp, P. Makk, S. Blanter, M. Weiss, K. Watanabe, T. Taniguchi, S. Csonka, and C. Schönenberger, Appl. Phys. Lett. **107**, 183108 (2015).
15. C. Forsythe, X. Zhou, T. Taniguchi, K. Watanabe, A. Pasupathy, P. Moon, M. Koshino, P. Kim, and C.R. Dean, (2017).
16. S.M. Gilbert, G. Dunn, A. Azizi, T. Pham, B. Shevitski, E. Dimitrov, S. Liu, S. Aloni, and A. Zettl, Sci. Rep. **7**, 15096 (2017).
17. A. Sinitskii, K.J. Erickson, W. Lu, A.L. Gibb, C. Zhi, Y. Bando, D. Golberg, A. Zettl, and J.M. Tour, ACS Nano **8**, 9867 (2014).
18. K.J. Erickson, A.L. Gibb, A. Sinitskii, M. Rousseas, N. Alem, J.M. Tour, and A.K. Zettl, Nano Lett. **11**, 3221 (2011).
19. C.-H. Park and S.G. Louie, Nano Lett. **8**, 2200 (2008).
20. M.Y. Han, B. Özyilmaz, Y. Zhang, and P. Kim, Phys. Rev. Lett. **98**, 206805 (2007).
21. S. Liu, B. Lu, Q. Zhao, J. Li, T. Gao, Y. Chen, Y. Zhang, Z. Liu, Z. Fan, F. Yang, L. You, and D. Yu, Adv. Mater. **25**, 4549 (2013).
22. J. Feng, K. Liu, R.D. Bulushev, S. Khlybov, D. Dumcenco, A. Kis, and A. Radenovic, Nat. Nanotechnol. **10**, 1070 (2015).
23. S. Garaj, S. Liu, J.A. Golovchenko, and D. Branton, Proc. Natl. Acad. Sci. **110**, 12192 (2013).
24. M.D. Fischbein and M. Drndić, Appl. Phys. Lett. **93**, 113107 (2008).
25. S.P. Surwade, S.N. Smirnov, I. V. Vlassiouk, R.R. Unocic, G.M. Veith, S. Dai, and S.M. Mahurin, Nat. Nanotechnol. **10**, 459 (2015).
26. D. Cohen-Tanugi and J.C. Grossman, Nano Lett. **12**, 3602 (2012).
27. K.K. Kim, A. Hsu, X. Jia, S.M. Kim, Y. Shi, M. Hofmann, D. Nezich, J.F. Rodriguez-Nieva, M. Dresselhaus, T. Palacios, and J. Kong, Nano Lett. **12**, 161 (2012).
28. W. Regan, N. Alem, B. Alemán, B. Geng, Ç. Girit, L. Maserati, F. Wang, M. Crommie, and A. Zettl, Appl. Phys. Lett. **96**, 113102 (2010).
29. V. Iberi, L. Liang, A. V. Ievlev, M.G. Stanford, M.-W. Lin, X. Li, M. Mahjouri-Samani, S. Jesse, B.G. Sumpter, S. V. Kalinin, D.C. Joy, K. Xiao, A. Belianinov, and O.S. Ovchinnikova, Sci. Rep. **6**, 30481 (2016).
30. Y. Deng, Q. Huang, Y. Zhao, D. Zhou, C. Ying, and D. Wang, (2016).
31. D. Emmrich, A. Beyer, A. Nadzeyka, S. Bauerdick, J.C. Meyer, J. Kotakoski, and A. Gölzhäuser, Appl. Phys. Lett. **108**, 163103 (2016).